

Clustering Future Scenarios Based on Predicted Range Maps

Davidow, Matthew Merow, Cory Che-Castaldo, Judy Schafer, Toryn L. J.
Düker, Marie-Christine Corcoran, Derek, Matteson, David S.

November 2020

Summary

1. Predictions of biodiversity trajectories under climate change are crucial in order to act effectively in maintaining the diversity of species. In many ecological applications, future predictions are made under various global warming scenarios as described by a range of different climate models. The outputs of these various predictions call for a reliable interpretation.
2. We propose a interpretable and flexible two step methodology to measure the similarity between predicted species range maps and cluster the future scenario predictions utilizing a spectral clustering technique.
3. We find that clustering based on ecological impact (predicted species range maps) is mainly driven by the amount of warming. We contrast this with clustering based only on predicted climate features, which is driven mainly by climate models.
4. The differences between these clusterings illustrate that it is crucial to incorporate ecological information to understand the relevant differences between climate models. The findings of this work can be used to better synthesize forecasts of biodiversity loss under the wide spectrum of results that emerge when considering potential future biodiversity loss.

Key-words: biodiversity; clustering; similarity measures; future scenarios; animal species; climate change.

1 Introduction

Predicting ecological responses to a rapidly changing climate is essential to enact effective conservation policies (Parry et al., 2007; Hannah et al., 2013, 2020). Future range maps of various species can be predicted based on predicted future patterns of climate (Burrows et al., 2014; Jones and Cheung, 2015; Molinos et al., 2016). However, predicting future patterns of climate is a challenging task due to the many sources of

uncertainty, and a plethora of climate predictions are possible that are consistent with various unknown factors (e.g. differing human policy responses, climate models). We are interested in the analysis of comparing the outputs of these various predictions and deducing common patterns among predictions.

We make use of climate predictions from the Coupled Model Intercomparison Project 6 (CMIP6). This project provides multiple climate predictions which vary by the underlying global climate model (GCM) and what representative concentration pathway (RCP) is used. An RCP is a greenhouse gas concentration trajectory (Eyring et al., 2016). Four such trajectories are included in CMIP6, varying in the quantity of greenhouse gas emissions to capture the uncertainty of future emissions. We refer to the RCP trajectory of least emission as “optimistic”, and refer to the most pessimistic trajectory as the “extreme” scenario. In this work we refer to a *scenario* as a (GCM, RCP) pair, these scenarios represent uncertainty both in the evolution of climate, and in future greenhouse gas emissions.

In order to interpret the differences among climate predictions, we propose a methodology to cluster the scenarios. We create such a clustering both from the climate features, and from predicted range maps for 1101 mammalian species. These predicted range maps are based on the predicted climate features, the details of these range maps are discussed in Section 2. These clusterings reveal the important differences between climate models, such as whether the global climate model or the RCP differences are the most salient features. The clustering will also group the scenarios into interpretable collections, such as an “optimistic” collection of scenarios of lesser ecological impact, and an “extreme” collection of scenarios of greater ecological impact.

Clustering the scenarios based on these predicted range maps is a difficult task due to the discrete and high dimensional nature of the range maps. Although Principal Component Analysis (PCA) is a common tool to analyze data, it has two significant drawbacks in this setting. One is that PCA implicitly measures distance between range maps in Euclidean space, whereas we present a flexible alternative, allowing for any similarity or distance between range maps. Secondly, it is not clear how to incorporate information from multiple species into a PCA-based approach.

Currently, a popular metric of change in species richness due to climate change is climate velocity (Burrows et al., 2014; Jones and Cheung, 2015; Molinos et al., 2016). However, these climate velocities rely heavily on climate information while ignoring ecological data. Such ecological information, such as species’ exposure to climate conditions not found in their current niches, are important factors to predict the species future ranges (Trisos et al., 2020). We incorporate such ecological data by clustering based on predicted range maps based on models of historical ranges.

We will contrast this ecologically driven clustering with a climate driven clustering to emphasise the importance of incorporating ecological information. This climate driven clustering will use only predicted climate features taken from CMIP6, such as annual mean temperature and annual mean precipitation. By

comparing the climate driven clustering and the ecological one obtained from the range map similarities, we demonstrate the need for incorporating ecological information. Clustering based only on climate features is a similar but distinct task to the ecological based clustering; the climate features are continuous whereas the ecological range maps are binary. Previously these scenarios have been clustered using the climate features by averaging these climate features over global regions Giorgi and Francisco (2000); Cannon (2015). However, spatially averaging the climate features this way loses significant information about the spatial variability of the features.

We propose a flexible two step approach to cluster both predicted species range maps and predicted climate features. The first step is to measure the pairwise similarity between the prediction maps. The second step is to use the pairwise similarities for spectral clustering, whose implementation is discussed in Section 2. This two-step procedure is highly flexible, any similarity measure can be used between range maps.

We propose to measure the similarity between range maps as the cosine similarity of the range maps. This choice allows for considerable flexibility; the modeller can weight absences and presences separately, and give certain sets of cells higher importance. In addition the cosine similarity is interpretable and comparable across species; it is always in the range $[-1, 1]$. This interpretability allows for a simple method to combine information across species, as will be discussed in Section 2.2.

2 Materials and Methods

We first describe prior modelling work to predict the future range maps given climate information. Then we discuss our methodology for clustering the scenarios; first based on on predicted range maps, and secondly based on predicted climate features. These clusterings reveal interpretable relationships between the scenarios, and the contrast of these two clusterings demonstrate the importance of incorporating ecological information.

2.1 Data: Predicted Range Map Modelling

A set of 9 GCMs are used from CMIP6 (Eyring et al., 2016; Stouffer et al., 2017), which span four different levels of RCPS. Five climate features are chosen from the set of 19 commonly used in WordCLIM (Fick and Hijmans, 2017), which were chosen to minimize correlations. These five climate features are annual mean temperature, temperature seasonality (standard deviation of temperature), annual precipitation, precipitation seasonality (standard deviation), and precipitation in the driest quarter of a year.

The five chosen climate features are used to fit a Poisson point process model to explain the present

day range maps (Merow et al., 2013; Elith et al., 2011). The present day occurrences of 1101 mammals are obtained from Miller (2020), whose range maps contain at 10 unique presence cells on a 10km grid. This Poisson point process model was used to predict future spatial occurrence based on these five predicted climate values. Binary maps are obtained from these abundance maps by thresholding based on the 5th percentile of predicted values at training presences. This approach is used to make predictions on all 1101 mammals using the 34 different sets of predicted climate features. We make use of these predicted range maps to measure the similarities between the 34 different climate scenarios.

2.2 Range Map Clustering Methodology

We present a novel methodology to cluster scenarios based on the binary presence maps such as those shown in Figure 1b. We now discuss the procedure for achieving this scenario clustering. This clustering illuminates the important similarities between scenarios, for instance if GCM or RCP is the main differentiating feature among scenarios, and additionally gives insight into the variation among scenarios.

2.2.1 Range Map Notation

For notational simplicity we focus the presentation of the methodology on a single species. Furthermore, we suppose our maps are on a n_r by n_c grid represented as $(r, c) : r = 1, \dots, n_r, c = 1, \dots, n_c$. We denote B_s as the binary presence map of this species according to scenario s , to be more precise $B_s(r, c) = 1$ if the cell at (r, c) represents a presence, and $B_s(r, c) = 0$ otherwise. We recognize it is important to consider how these range maps differ from the present day as will be discussed further. For this reason we denote by P the present day map. Similarly as for $B(r, c)$, we write $P(r, c) = 1$ if the cell at (r, c) is presently occupied, and 0 otherwise. We let the binary map A (same size as P and each B_s) denote the background set, where valid absences may occur. For instance, the set A can take the value 1 only when there is land, or alternatively only on the same continent or regional areas as P . We have chosen to take A as the union of the original map and all scenarios, thus $A(r, c) = 1$ if $P(r, c) = 1$, or there is a scenario s such that $B_s(r, c) = 1$.

2.2.2 Cosine Similarity

In order to interpret the differences between range map predictions, a similarity or distance measure is called for between pairs of range maps. The quantification of the similarity or distance between range maps allows us to cluster the scenarios, which is a desirably interpretable result.

There exists a plethora of alternative measures to quantify the similarity or distance between these presence maps (Visser and De Nijs, 2006; Wilson, 2011; Hagen, 2002; Hill et al., 2013; Gritti et al., 2013).

The Hellinger distance and Kullback-Leibler divergence rely on a probabilistic interpretation, and thus it is difficult to incorporate absences into these measures (Wilson, 2011). The Kappa statistic (Hagen, 2002) can be used to measure similarities between categorical maps, however it is not as clear how to weight important cells, such as novel absences. In addition, the Kappa statistic does not directly incorporate the relative frequencies of absences and presences. For instance if two maps both predict all presences except a single absence cell, these two maps will have a negative Kappa statistic if their one absence cell differs. However, for our purposes we would like to consider such a pair of maps very similar. The Wasserstein distance (or Earth Mover’s Distance) (Peyré et al., 2019; Kranstauber et al., 2017) is an attractive alternative which captures the idea of movement of a species. However, the Wasserstein distance does not model the disappearance of regions (as opposed to the shift/movement of regions), and computing the distance via optimal discrete transport (a linear program of quadratic size in the number of present cells) proved too slow or even infeasible (no solution found to the linear program) in all but the smallest maps (the maps with the smallest number of presence cells).

We chose the cosine similarity function, which has several attractive features. It is flexible; the modeller can weight absences and presences separately, and the modeller has the flexibility to give certain sets of cells higher importance. The cosine similarity is interpretable and comparable across species as we describe below.

We compute the pairwise similarity between range maps as the cosine similarity of their weighted range maps. The motivation and details for weighting the range maps is discussed in Section 2.2.3. In short, we construct a weighted map W_s based on the binary range map B_s and present day map, P . For a pair of scenarios s, s' with corresponding binary range maps $B_s, B_{s'}$ and present day map P , we measure their similarity as the cosine similarity of their weighted maps, $\text{CS}(W_s, W_{s'})$. We suppose that a map G on an n_r by n_c grid can be interpreted as a vector with length $n_r \times n_c$. Then the cosine similarity between two vectors $W_s, W_{s'}$ can be written as

$$\text{CS}(W_s, W_{s'}) = \frac{W_s \cdot W_{s'}}{\|W_s\|_2 \|W_{s'}\|_2} = \frac{\sum_{r=1}^{n_r} \sum_{c=1}^{n_c} W_s(r, c) W_{s'}(r, c)}{\|W_s\|_2 \|W_{s'}\|_2}, \quad \text{with} \quad \|W_s\|_2 = \left(\sum_{r=1}^{n_r} \sum_{c=1}^{n_c} W_s(r, c)^2 \right)^{1/2}. \quad (1)$$

2.2.3 Weighted Map

Weighting the cells of the binary maps is required to quantitatively measure the similarity between range maps. For each scenario s , we denote the corresponding weighted map W_s . The value of $W_s(r, c)$ is 0 if $A(r, c) = 0$, but when $A(r, c) = 1$ we choose one of four values for $W_s(r, c)$ depending on whether the cell

represents a presence/absence for the present day, and a presence/absence for the scenario. These four choices are shown in Table 1.

	$P(r, c) = 1$	$P(r, c) = 0$
$B(r, c) = 1$	p_{keep}	p_{new}
$B(r, c) = 0$	a_{new}	a_{keep}

Table 1: Cell Weighting Values for $W(r, c)$ given $A(r, c) = 1$.

The choice of weightings in Table 1 is dependent on the use of cosine similarity. For instance using cosine similarity but representing presences with the value 1 and absences with 0 is inappropriate because any two maps will have positive similarity, and this choice will also have the property that absences and presences are counted differently in the denominator of the cosine similarity.

These first four cases (reading row by row) represent unchanged (kept) presences, new presences, new absences, and unchanged absences respectively, where “keep” and “new” are with respect to the present day distribution, P . For example, a cell corresponding to p_{keep} is a cell that is present in P , and is kept present according to scenario B_s . Presences are given positive weights, absences negative weights, and we choose $|a_{\text{new}}| > |a_{\text{keep}}|$, to emphasize those cells whose ecological suitability for this species is vanishing. These “lost” cells corresponding to novel absences are particularly important; they represent cells where the climate is changing so drastically that the species cannot continue to live there. In addition these cells should be weighted higher because we are more confident about their prediction; by definition they exist within the training data’s presences. By contrast the cells corresponding to p_{new} represent regions where the species are predicted to move to, however such predictions are more uncertain as the movement of a species is complex and not directly taken into account by the Poisson point process model. Thus we also make the choice $|p_{\text{keep}}| > |p_{\text{new}}|$. We make the choice $|a_{\text{new}}| = |p_{\text{keep}}| = 1, |a_{\text{keep}}| = |p_{\text{new}}| = 0.5$ to represent the fact we are more confident about all cells in the region of present day occurrences (those cells corresponding to $P(r, c) = 1$). However, we emphasize the flexibility of our model, alternative choices can be made depending on the modeler’s goals. A visualization of this weighting scheme is shown in Figure 1.

The computation and resultant cosine similarity using these weighted maps are highly interpretable; when two scenarios agree on the presence or absence of a cell, this cell has a positive contribution to the cosine similarity, whereas the cell has a negative contribution when the two scenarios disagree. The resulting similarity is always in the range $[-1, 1]$ (for any choice of weightings), and takes the value 1 when the two maps are identical and -1 if the two maps completely disagree on presences, as long as $|a_{\text{new}}| = |p_{\text{keep}}|, |a_{\text{keep}}| = |p_{\text{new}}|$, which was argued for previously.

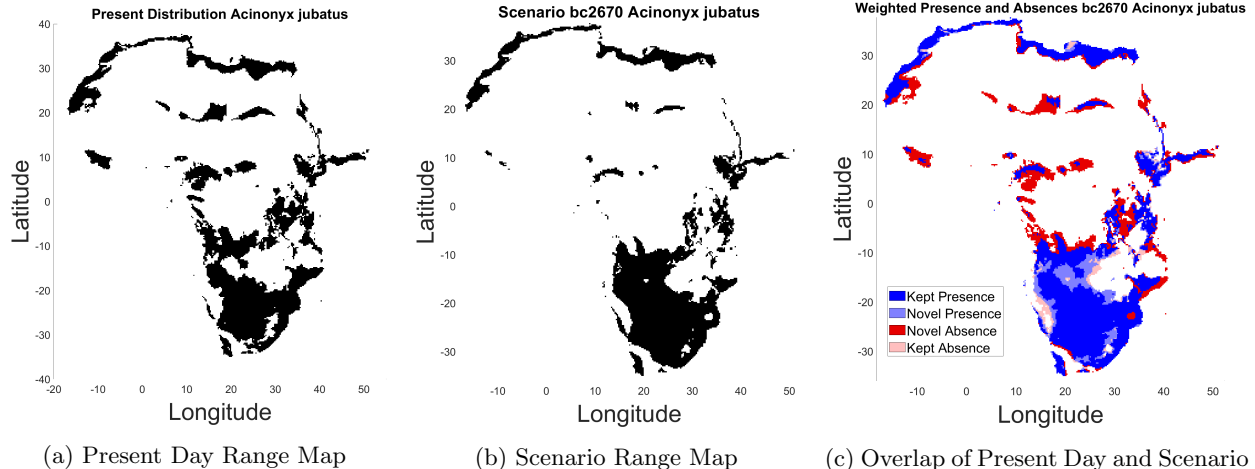


Figure 1: Illustration for weighted presences and absences. Presences are shown in blue, absences in red/pink. The overlap with the present day is shown in darker regions which represent more significant cells, which are dark blue kept presences, and dark red new absences, which represent “lost” cells. A strength of our proposed methodology is the flexibility to weight these cells differently

2.2.4 Spectral Clustering

For all species we compute the pairwise scenario similarity matrix by computing the cosine similarity, eq. (1) on each pair of scenarios. That is for each species m , we construct the n_s -by- n_s matrix $S^m(s, s') = CS(W_s^m, W_{s'}^m)$, where n_s is the number of scenarios and W_s^m is the weighting map for species m on scenario s . Spectral clustering is well suited to cluster the scenarios based on this similarity measure (Von Luxburg, 2007).

The properties of spectral clustering are understood from a graph theory perspective. The similarity matrix S^m can be thought of as an undirected graph whose nodes are the scenarios and edge weights between a pair of scenarios s and s' given by $S^m(s, s')$. Spectral clustering has best performance on sparse graphs, thus for the dense similarity matrix S^m , the first step is to sparsify it by means of taking the k -nearest neighbor graph, that is retaining an edge from s to s' only if s' is within the top k neighbors of s (i.e. it is within the top k nodes of maximal similarity to s). However this would lead to a directed graph as this definition of nearest neighbor is not symmetric. Thus we retain the undirected edge from s to s' if either s' is within the top k neighbors of s , or vice-versa. The retained edges are still weighted by the similarity of their endpoints. We denote by E this matrix of retained weights.

The main tool of spectral clustering is the graph Laplacian $L = D - E$, where D is a diagonal matrix of node degree, $D_{ii} = \sum_{j=1}^{n_s} E(i, j)$. We use the random-walk normalized graph Laplacian, $L_{rw} = D^{-1}L$ as suggested in Von Luxburg (2007). Both L and L_{rw} have several nice properties, they are positive semi-definite and the multiplicity of their zero eigenvalue is the number of connected components of the graph.

For most real-world graphs including the sparsified cosine similarity matrix E , the graph is fully connected and thus the number of connected components of this graph is one. When this is the case the eigenvectors corresponding to the smallest non-zero eigenvalues can be used as an embedding. This can be thought of from a perturbation perspective, if the graph had true clusters of connected components than these eigenvectors would have the same span as vectors representing clustering membership indicators. However in real world graphs there are a few “noisy” edges between clusters, thus these first few eigenvectors instead are near piecewise on those indicators.

Drawing from this insight, the space associated with the eigenvectors of L_{rw} , which we denote as columns of a matrix U , is used as “spectral embedding”. We use the second and third eigenvectors of U (corresponding to the second and third smallest eigenvalue) as the spectral embedding, that is scenario s is represented by $(U_{s,2}, U_{s,3})$. We choose a simple clustering algorithm, single-linkage clustering, to cluster in this embedded space as it performs well according to the Davies-Bouldin criterion, a common clustering criterion for how well separated clusters are (Davies and Bouldin, 1979).

This clustering can be performed for a single species using only S^m , for example this is performed for four different species, shown in Figure 6. These results will be discussed in the next section. One way to combine information across animals is to average the similarity matrices across all $n_m = 1101$ animals, as in $S = (1/n_m) \sum_{a=1}^{n_m} S^m$. Performing spectral clustering using this averaged similarity matrix, S , is shown in Figure 5b.

2.3 Global Spatial Diversity Loss: Data Summary Visualization

One can get an overall sense of the changes predicted in the range maps from Figure 2, which shows how the diversity of mammals is spread spatially throughout the globe. We see from both Figures 2c and 2d that significant diversity losses are predicted around the equator in South America and Africa, whereas there is some diversity increases further up north, consistent with previous findings (Chen et al., 2011).

2.3.1 Frequency Analysis

One way to qualitatively measure the performance of the clustering is to look at the spatial overlap of presences for each scenario. That is we define the frequency map F^m based on the scenario maps: $F^m(r, c) := \sum_{s=1}^{n_s} B_s^m(r, c)$ For example the overlap of all 34 scenarios for the African cheetah is shown in Figure 8a.

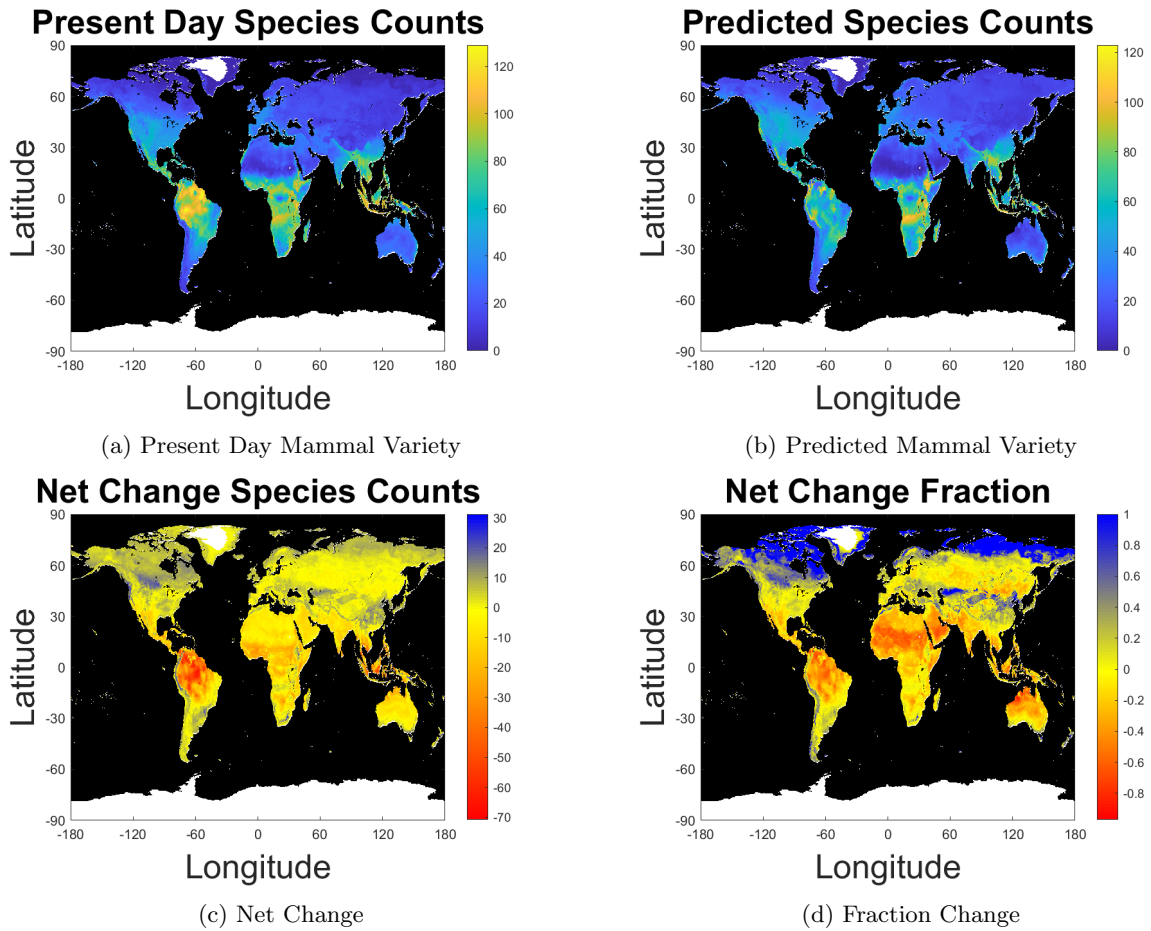


Figure 2: Visualization of the mammal richness in the dataset over space. White cells correspond to locations with no recorded presences. Our findings are consistent with Chen et al. (2011) which finds that species are moving poleward and towards higher elevations, there is loss around the equator and some increase in diversity towards the northern pole.

2.3.2 Principal Component Analysis

Principal component analysis is a great tool to understand the main directions of variation in data. We use PCA to visualize the correlations of presence cells. This can be performed for a single species by considering each scenario as an observation, with $n_r \times n_c$ binary features corresponding to the vectorized (flattened) binary range map.

2.3.3 Climate Based Scenario Clustering

We discuss the process of clustering using only the five climate features that were used to predict the range maps. This clustering when contrasted with the ecologically driven clustering demonstrates the importance of incorporating ecological information. Each of these five globally distributed features is predicted across the 34 scenarios. In order to directly compare to our ecologically based clustering, we utilize the climate features to perform a clustering in a similar fashion to the ecologically based clustering. However, for continuous data, the cosine similarity is not appropriate, as two maps that are scaled versions of each other would be considered very similar to each other, which is not desirable. For instance if one map predicted two degrees warmer everywhere than another, the cosine similarity between these two maps would very high, which is not desirable as these two maps represent significantly different predictions. Instead we use the L_2 distance between maps, which will effectively use both the difference between the means of maps, and differences in the spatial variation. To incorporate all five climate features, each feature is normalized before applying the L_2 distance. We denote $T_s^f(r, c)$ the value of feature f according to scenario s at location (r, c) . The feature scaled L_2 distance between a pair of scenarios s and s' using all five features is given by:

$$H(s, s') = \sum_{f=1}^5 \sum_{r=1}^{n_r} \sum_{c=1}^{n_c} [(T_s^f(r, c) - T_{s'}^f(r, c))/\sigma_f]^2.$$

Where σ_f is the standard deviation of feature f measured across all locations and scenarios, that is we calculate the mean of each feature across all locations and scenarios,

$$\sigma_f^2 = \sum_{s=1}^{n_s} \sum_{r=1}^{n_r} \sum_{c=1}^{n_c} [T_s^f(r, c) - \mu_f]^2 \quad \text{with} \quad \mu_f = (n_s \cdot n_r \cdot n_c)^{-1} \sum_{s=1}^{n_s} \sum_{r=1}^{n_r} \sum_{c=1}^{n_c} T_s^f(r, c). \quad (2)$$

Spectral clustering requires a similarity matrix (instead of a dissimilarity or distance matrix), thus we transform the pairwise L_2 distances into similarities with any monotonically negative function, such as $x \rightarrow 1/x$. An important step in spectral clustering is to sparsify the similarity matrix by keeping only the largest similarities (discussed above), and so any monotonically negative function will produce the same spectral embedding and clusters Von Luxburg (2007). Thus we use the similarity matrix $L(s, s') := 1/H(s, s')$

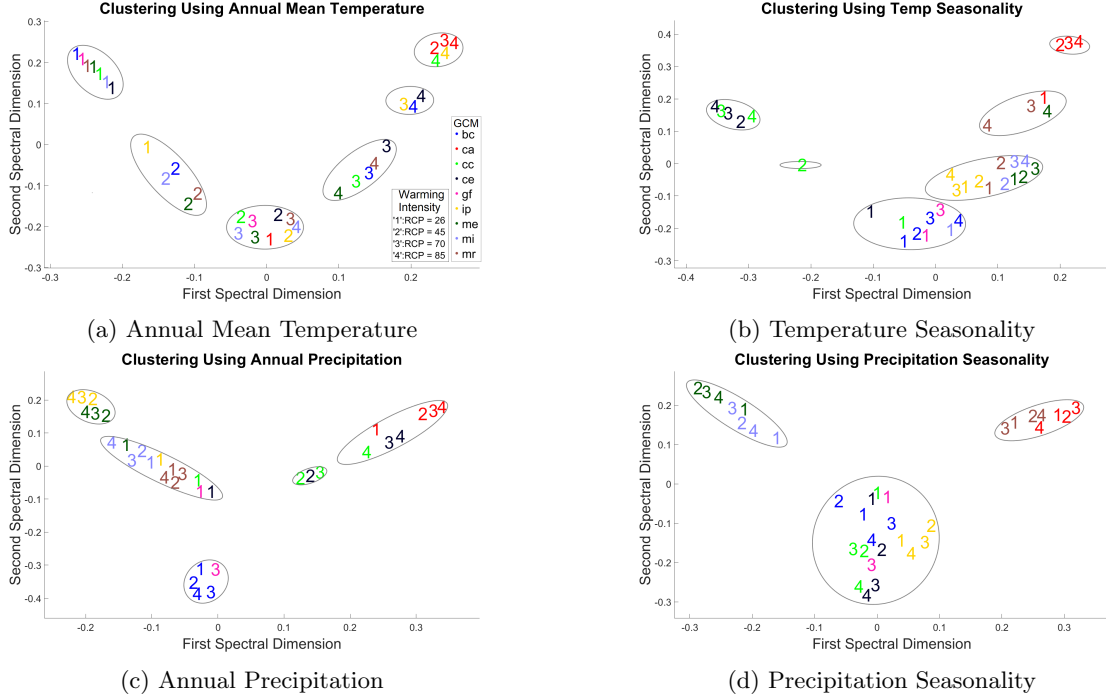


Figure 3: Spectral clustering of scenarios using individual climate features (one of the five is not shown due to space). The annual temperature clustering is most similar to the ecological clustering of Figure 5b, clustering mainly by RCP. The other features mainly cluster mainly by GCM. This is why the climate driven clustering of Figure 5a is driven mainly by GCM, most of the features are. The ecological clustering is important to discern which of these features are most ecologically relevant, these plots show that annual temperature contains the most ecologically relevant differences between climate models.

as the similarity matrix for spectral clustering, which is shown in Figure 5b.

2.4 Variation of Scenarios

We summarize some overall patterns of the projected range maps by counting both presences that differ from the present day range map, and absences that differ from the present day range maps (cells corresponding to a_{new} and p_{new} respectively). The fraction of each of these cell types is averaged over species for each scenario. The resulting average of fraction of a_{new} and p_{new} type cells is shown in Figure 4, which shows that these novel absences and novel presences are correlated.

3 Results and Discussion

In this section we discuss the scenario clusterings, with emphasis on the difference between the climate based and ecological based clustering. We then demonstrate that we have detected meaningful clusters, with range maps within clusters similar to each other, but different than range maps in other clusters.

3.1 Range Shifts

By comparing the fraction of cells corresponding to a_{new} and p_{new} we get a sense of the changes of the range maps compared to the present day range map. This is shown in Figure 4, which demonstrates these range maps tend to predict range shifts, as opposed to range expansions or contractions. We conclude this because the number of new presences and new absences grow together, which would occur as range shifts, instead of say absences growing as presences shrink, which would be indicative of an overall range decrease.

On average there are significantly more novel absences (average 38% (28% s.d.) of current range) than novel presences (average 25% (26% s.d.)), which implies that the species ranges are shrinking (average 13% net loss, (31% s.d.)) due to the changing climate.

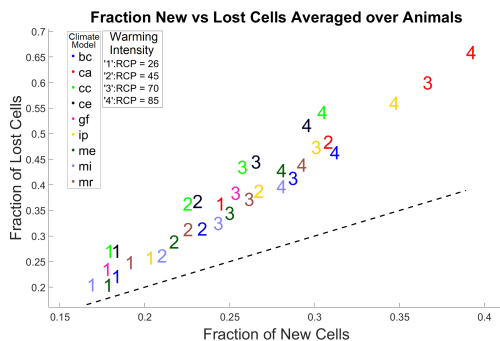


Figure 4: Shows that predicted range maps tend to be shifted, that is lost and new cells grow together, with losses being larger than gains, as the scenarios are above the 45 degree dashed black line.

3.2 Clustering Plots

The spectral clustering results using the species specific similarity matrix is shown in Figure 6 for four species, illustrating the main types of patterns observed. We see an interesting mix of RCP and GCM dependence. It appears that RCP is a major driving factor that separates these clusters; in most of these clusterings the far left (“optimistic”) cluster contains mainly scenarios with low RCP, and the far right (“extreme”) cluster only scenarios with high RCP. However, the clustering using the slender treeshew (*Tupaia gracilis*) is driven mainly by GCM. This clustering mainly by GCM was found in many species (30%), although the most common trend is RCP dependence (70% of species). The variability among animals is further evidence supporting the importance of the climate ecology relationship: the most important difference between climate models (GCM or RCP) varies depending on the individual species’ response to the climate.

The spectral cluster results from using the similarity matrix averaged over all 1101 mammals is shown in Figure 5b. We see in the bottom cluster of Figure 5b an interesting mix of varying RCP and GCM. This suggests that RCP alone does not account for the variation, the GCM is also important. However, there

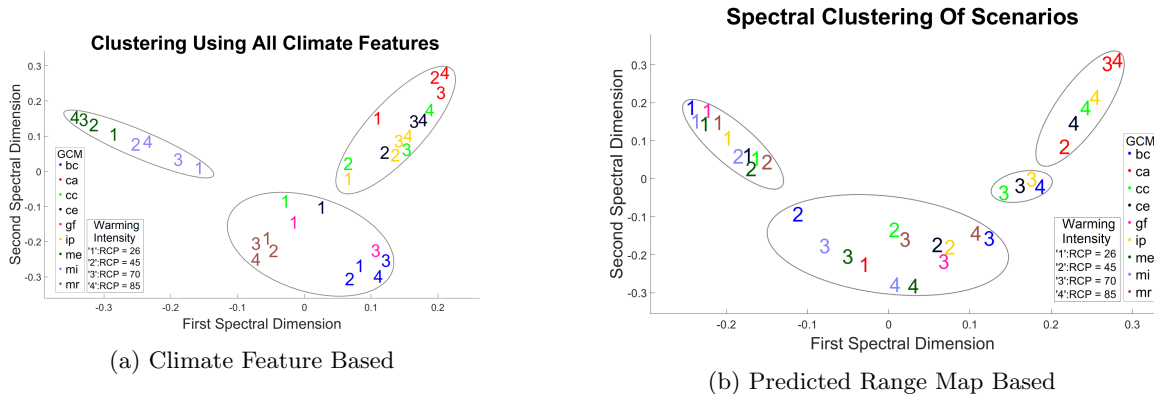


Figure 5: In the climate based clustering shown on the left, the clusters are mainly determined by GCM. This clustering is significantly different from the ecological based one shown on the right, which demonstrates the importance of incorporating ecological information. B: Scenario Embedding and Clustering. The clusters are mainly driven by RCP. However, there is still some relationships among the GCM, for instance the red 'ca' GCM predicts more extreme outcomes, and at each level of RCP the green black and yellow (cc,ce,ip) climate models are together. This clustering is significantly different from the climate based one (Panel A), which demonstrates the importance of incorporating ecological information.

are still variabilities among the GCMs. For example, the “ca” climate model appears twice in the far right cluster.

Instead of averaging over all species, we also performed clustering for only the species most at risk, defined by those species whose fraction of area lost is among the highest 10%. This loss in area can be used to approximate a loss in population abundance using the techniques in He (2012); Che-Castaldo and Neel (2016). Performing spectral clustering by using the average of similarity matrices of this subset of animals at risk is shown in Figure 7. This clustering puts a stronger emphasis on RCP, that is, the animals most at risk are more sensitive to RCP.

3.3 Cluster Quality Analysis

One way to qualitatively measure the performance of the clustering is to look at the spatial overlap of presences for each scenario. For example the overlap of all 34 scenarios is shown in Figure 8a. We see that the cluster associated with the smallest RCP scenarios (“optimistic” scenarios) accounts for most of the presences in the discrepant regions, whereas the cluster associated with the highest RCP (“extreme” scenarios) accounts for many of the absences. This demonstrates that we have discovered meaningful clusters; there is agreement within clusters but disagreements across clusters.

We visualize the correlations of presence cells over scenarios using principal component analysis. This can be performed for a single species by considering each scenario as an observation, with $n_r \times n_c$ binary features corresponding to the vectorized (flattened) binary range map. Performing PCA in this way is shown

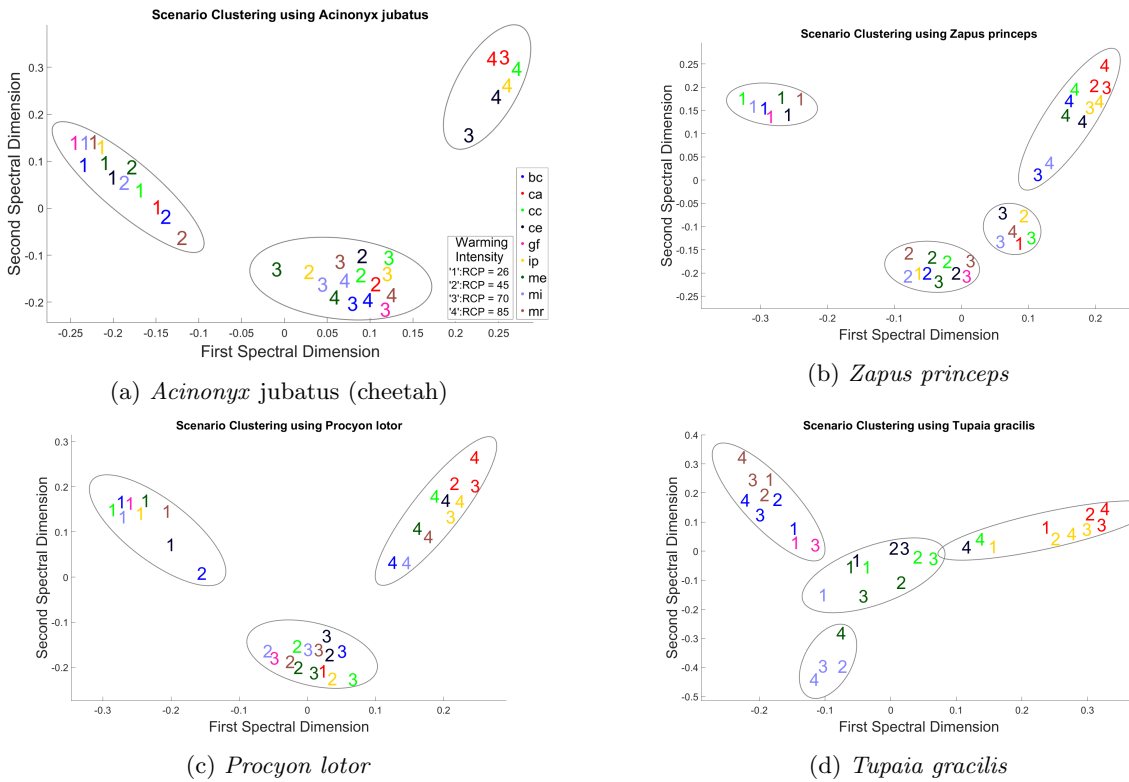


Figure 6: Spectral clustering of scenarios using individual species. We see mainly grouping by RCP for the first three, but a starkly differently mainly GCM driven clustering for the treeshrew. This variety was found among animals, most species driven clusterings are strongly connected with RCP, but some are more connected with GCM. These differences between species further demonstrates that ecological information is important to interpret the differences between scenarios.

Clustering by Species Most at Risk

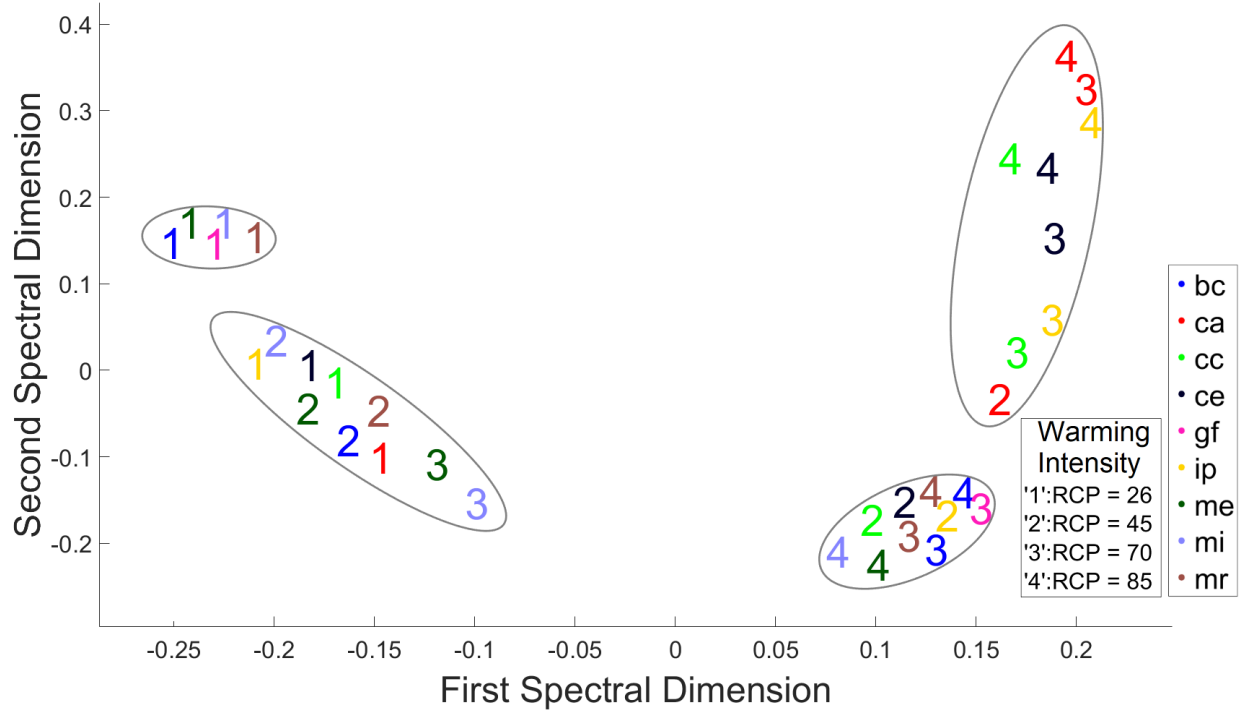


Figure 7: Scenario Embedding and Clustering using only animals in riskiest quantiles. Clustering based only on these species most at risk puts an even higher emphasis on RCP than the clustering in Figure 5b. This further demonstrates the importance of accounting for ecological information, as different subsets of ecological populations emphasize RCP even more strongly.

for the cheetah in Figure 8b. The mix of positive and negative coordinates illustrates the fact that the most extreme scenarios do not only “lose” certain cells, but also predict novel presences.

3.4 Individual Climate Feature Clustering

We see that the climate based clustering is significantly different than the ecological one, as the clustering is driven mainly by GCM instead of by RCP in the ecological based clustering. This is evidence for the importance of considering the specific climate niche occupied by a species in relation to how those conditions are projected to change. Although these same five features are used to predict the ecological range maps, these predicted range maps paint a different picture of the scenario clustering because of how the animals are influenced by the climate features. In fact, we can get a sense of feature importance by clustering based on individual climate features, shown in Figure 3. We see that clustering using only the annual temperature creates the most similar clustering to the ecologically driven one, suggesting that annual temperature is the most important feature of these five.

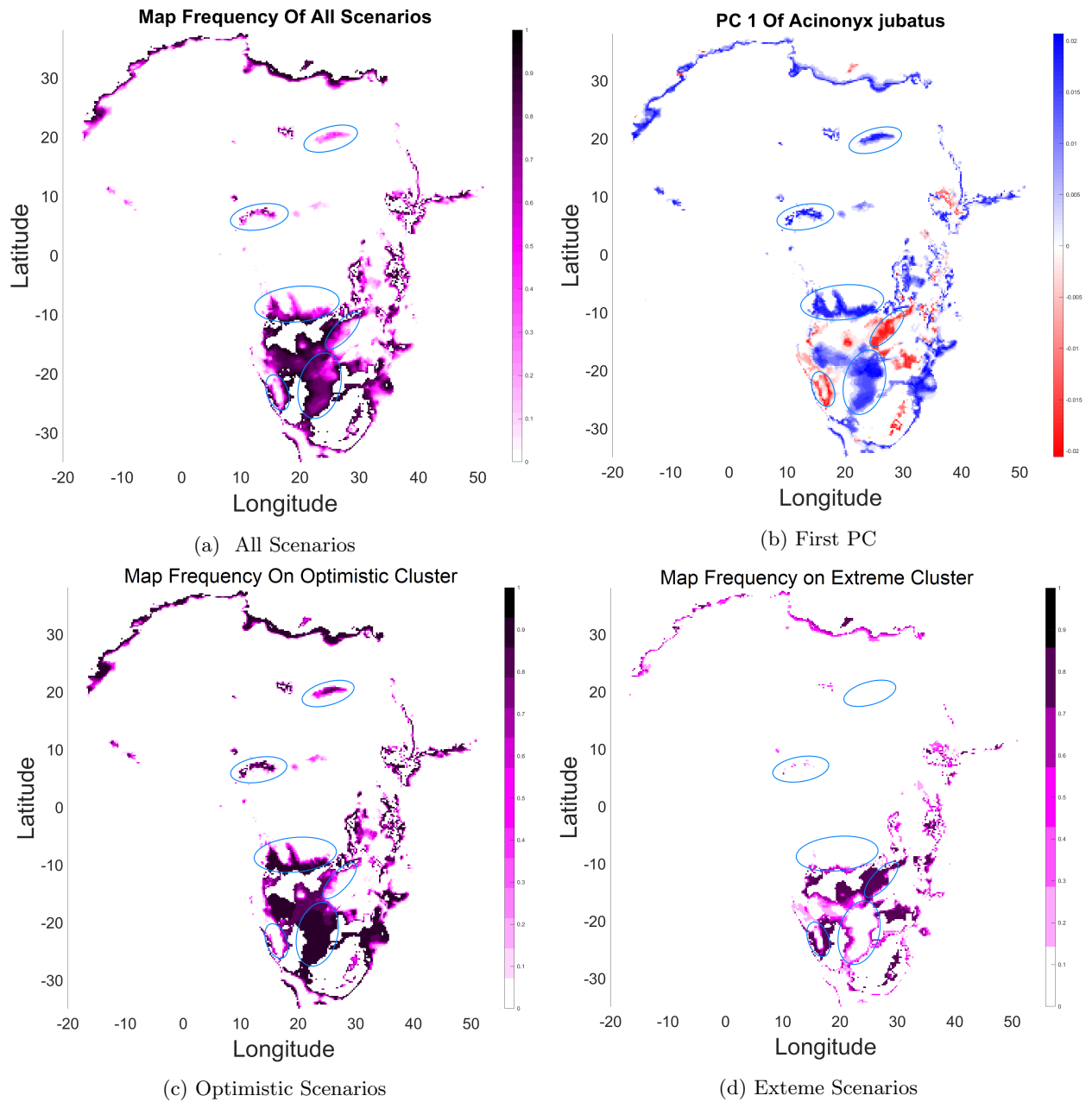


Figure 8: Sum of presences over scenarios. A meaningful clustering should have strong similarities within cluster, and differences across cluster. The circled regions showed that indeed we have discovered meaningful clusters; there is agreement within cluster in these regions, but differences across clusters.

4 Conclusion

We have proposed a novel methodology to cluster scenarios based on ecological range maps. The presented approach is interpretable, flexible, and fast. We have demonstrated different patterns of clustering depending on which subsets of species are included. For instance, the animals most at risk group many of the higher RCP scenarios together. The differences between the climate based clustering and ecological based clustering highlights the importance of considering ecological response; the interaction of climate and ecology is essential to understand the ecologically most important differences between future scenario predictions. An interesting direction to explore further is to uncover subsets of animals that respond differently than others. For instance it may be the case that rodents tend to fare worse under the “bc” climate model, compared to other mammals. A similar area of future research is to determine why some species like the slender treesheep cluster more by GCM instead of the more pattern of RCP. Are these species less sensitive to temperature changes? Another extension is to consider how to combine information across animals in a more holistic manner. For instance, Dong et al. (2013) presents a methodology to cluster according to many graphs, which could be applied in our use case to the scenario graphs from each species.

References

- Martin L Parry, Osvaldo Canziani, Jean Palutikof, Paul Van der Linden, and Clair Hanson. *Climate change 2007-impacts, adaptation and vulnerability: Working group II contribution to the fourth assessment report of the IPCC*, volume 4. Cambridge University Press, 2007.
- Lee Hannah, Makihiko Ikegami, David G Hole, Changwan Seo, Stuart HM Butchart, A Townsend Peterson, and Patrick R Roehrdanz. Global climate change adaptation priorities for biodiversity and food security. *PLoS one*, 8(8):e72590, 2013.
- Lee Hannah, Patrick R Roehrdanz, Pablo A Marquet, Brian J Enquist, Guy Midgley, Wendy Foden, Jon C Lovett, Richard T Corlett, Derek Corcoran, Stuart HM Butchart, et al. 30% land conservation and climate action reduces tropical extinction risk by more than 50%. *Ecography*, 2020.
- Michael T Burrows, David S Schoeman, Anthony J Richardson, Jorge Garcia Molinos, Ary Hoffmann, Lauren B Buckley, Pippa J Moore, Christopher J Brown, John F Bruno, Carlos M Duarte, et al. Geographical limits to species-range shifts are suggested by climate velocity. *Nature*, 507(7493):492–495, 2014.
- Miranda C Jones and William WL Cheung. Multi-model ensemble projections of climate change effects on global marine biodiversity. *ICES Journal of Marine Science*, 72(3):741–752, 2015.

- Jorge García Molinos, Benjamin S Halpern, David S Schoeman, Christopher J Brown, Wolfgang Kiessling, Pippa J Moore, John M Pandolfi, Elvira S Poloczanska, Anthony J Richardson, and Michael T Burrows. Climate velocity and the future global redistribution of marine biodiversity. *Nature Climate Change*, 6(1): 83–88, 2016.
- Veronika Eyring, Sandrine Bony, Gerald A Meehl, Catherine A Senior, Bjorn Stevens, Ronald J Stouffer, and Karl E Taylor. Overview of the coupled model intercomparison project phase 6 (CMIP6) experimental design and organization. *Geoscientific Model Development*, 9(5):1937–1958, 2016.
- Christopher H Trisos, Cory Merow, and Alex L Pigot. The projected timing of abrupt ecological disruption from climate change. *Nature*, 580(7804):496–501, 2020.
- Filippo Giorgi and Raquel Francisco. Uncertainties in regional climate change prediction: a regional analysis of ensemble simulations with the hadcm2 coupled aogcm. *Climate Dynamics*, 16(2-3):169–182, 2000.
- Alex J Cannon. Selecting gcm scenarios that span the range of changes in a multimodel ensemble: application to cmip5 climate extremes indices. *Journal of Climate*, 28(3):1260–1267, 2015.
- Ronald J Stouffer, Veronika Eyring, Gerald A Meehl, Sandrine Bony, Cath Senior, Bjorn Stevens, and KE Taylor. CMIP5 scientific gaps and recommendations for CMIP6. *Bulletin of the American Meteorological Society*, 98(1):95–105, 2017.
- Stephen E Fick and Robert J Hijmans. Worldclim 2: new 1-km spatial resolution climate surfaces for global land areas. *International journal of climatology*, 37(12):4302–4315, 2017.
- Cory Merow, Matthew J Smith, and John A Silander Jr. A practical guide to maxent for modeling species’ distributions: what it does, and why inputs and settings matter. *Ecography*, 36(10):1058–1069, 2013.
- Jane Elith, Steven J Phillips, Trevor Hastie, Miroslav Dudík, Yung En Chee, and Colin J Yates. A statistical explanation of maxent for ecologists. *Diversity and distributions*, 17(1):43–57, 2011.
- Joe Miller. Gbif home page, 2020. URL <https://www.gbif.org>.
- Hans Visser and T De Nijs. The map comparison kit. *Environmental Modelling & Software*, 21(3):346–358, 2006.
- Peter D Wilson. Distance-based methods for the analysis of maps produced by species distribution models. *Methods in Ecology and Evolution*, 2(6):623–633, 2011.
- Alex Hagen. Multi-method assessment of map similarity. In *Proceedings of the 5th AGILE Conference on Geographic Information Science*, pages 171–182. Universitat de les Illes Balears Palma, Spain, 2002.

- Mark O Hill, Colin A Harrower, and Christopher D Preston. Spherical k-means clustering is good for interpreting multivariate species occurrence data. *Methods in Ecology and Evolution*, 4(6):542–551, 2013.
- Emmanuel S Gritti, Anne Duputie, Francois Massol, and Isabelle Chuine. Estimating consensus and associated uncertainty between inherently different species distribution models. *Methods in Ecology and Evolution*, 4(5):442–452, 2013.
- Gabriel Peyré, Marco Cuturi, et al. Computational optimal transport: With applications to data science. *Foundations and Trends® in Machine Learning*, 11(5-6):355–607, 2019.
- Bart Kranstauber, Marco Smolla, and Kamran Safi. Similarity in spatial utilization distributions measured by the earth mover’s distance. *Methods in Ecology and Evolution*, 8(2):155–160, 2017.
- Ulrike Von Luxburg. A tutorial on spectral clustering. *Statistics and computing*, 17(4):395–416, 2007.
- David L Davies and Donald W Bouldin. A cluster separation measure. *IEEE transactions on pattern analysis and machine intelligence*, 2(2):224–227, 1979.
- I-Ching Chen, Jane K Hill, Ralf Ohlemüller, David B Roy, and Chris D Thomas. Rapid range shifts of species associated with high levels of climate warming. *Science*, 333(6045):1024–1026, 2011.
- Fangliang He. Area-based assessment of extinction risk. *Ecology*, 93(5):974–980, 2012.
- Judy P Che-Castaldo and Maile C Neel. Species-level persistence probabilities for recovery and conservation status assessment. *Conservation Biology*, 30(6):1297–1306, 2016.
- Xiaowen Dong, Pascal Frossard, Pierre Vandergheynst, and Nikolai Nefedov. Clustering on multi-layer graphs via subspace analysis on Grassmann manifolds. *IEEE Transactions on signal processing*, 62(4):905–918, 2013.